



*Araştırma Makalesi / Research Article*

## Low Velocity Impact Damage Response Of Carbon Fiber Reinforced Composites At Low Temperatures

*Karbon Fiber Takviyeli Kompozitlerin Düşük Sıcaklıklarda Düşük Hızdaki Darbe Dayanımı*

Zafer Özdemir<sup>1\*</sup>, Osman Selim Türkbaş<sup>2</sup> and Dilara Yılmaz<sup>3</sup>

<sup>1</sup>Balıkesir University, Engineering Faculty, Mechanical Engineering Department, 10100, Balıkesir, Turkey.

<sup>2</sup>Gazi University, Engineering Faculty, Mechanical Engineering Department, 06400, Ankara, Turkey.

<sup>3</sup>Gazi University, Engineering Faculty, Mechanical Engineering Department, 06400, Ankara, Turkey.

### ARTICLE INFO

#### Article History

Received 09.10.2019

Revised 01.12.2019

Accepted 27.12.2019

Available Online 31.12.2019

#### Keywords

Low Temperature, Low Velocity, Impact Response, Carbon Fiber Reinforced Composite, Strain

### MAKALE BİLGİSİ

#### Makale Tarihi

Alınış 09.10.2019

Revize 01.12.2019

Kabul 27.12.2019

Online Yayınlama 31.12.2019

#### Anahtar Kelimeler

Düşük Sıcaklık, Düşük Hız, Darbe Direnci, Karbon Fiber Takviyeli Kompozitler, Gerinim

### ABSTRACT

Carbon Fiber Reinforced Composite (CFRC) plates have been subjected to low energy impact tests at 22,5°C (with strain gauge mounted), 22,5°C, 0°C, -30°C and -60°C separately. CFU10T carbon is chosen as fiber material and CR80 epoxy resin as matrix. The samples have been prepared as 100 X 100 mm. width/length and 2 mm. (thickness), 8 layered respectively and have been orientated as quasi-isotropic. The plate samples have been prepared by hand layup method. Low velocity impact tests have been carried out by Weight Drop Impact Test Setup according to ASTM D7136. Critical response force-time, strain and damage response have been investigated. It has been observed that; as the temperature decreases, contact forces increase and contact time decreases. The laminate number and lay up orientation also affect the low impact energy behavior of plates. As the temperature decreases, impact strength of CFRP plates decreases. It has been experimentally observed and proved that low temperature decreases impact strength.

### ÖZ

Karbon fiber takviyeli kompozitler (KFTK); 22,5°C (strain-gage li), 22,5°C, 0°C, -30°C ve -60°C sıcaklıklarda düşük enerjili darbe testlerine tabi tutulmuşlardır. CFU10T karbon fiber ve CR80 reçine matriks malzeme olarak kullanılmıştır. Numuneler 100 X 100 mm. genişlik/uzunluk ve 2 mm. kalınlıkta 8 tabakalı olarak hazırlanmış ve quasi-isotropic olarak ayrı ayrı yönlendirilmişlerdir. Tabakalar el yapımı yayma metodu ile hazırlandıktan sonra ASTM D7136'ya göre düşük hızda darbe testine tabii tutulmuşlardır. Kritik kuvvet-zaman, gerinim-zaman grafikleri hazırlanarak ayrı ayrı hasar analizleri yapılmıştır. Sıcaklık azaldıkça temas kuvvetinin arttığı ve temas zamanının azaldığı gözlemlenmiştir.

#### \*Corresponding Author

E-mail adress: [ozdemirzafer@yahoo.com](mailto:ozdemirzafer@yahoo.com) (Zafer Özdemir), [turkbaz@gazi.edu.tr](mailto:turkbaz@gazi.edu.tr) (Osman Selim Türkbaş), [dlrylmz@gmail.com](mailto:dlrylmz@gmail.com) (Dilara Yılmaz)

## 1. INTRODUCTION

Fiber-reinforced composites have been used as engineering materials for nearly five decades. Early development of fiber-reinforcement composite technology began in the defense sector where uses for composites included such things as filament-wound rocket motor cases. Evaluation of the technology took place primarily in the defense industry for many years due mainly to the extremely high costs associated with developing and manufacturing these materials. As technology matured, development costs decreased to the point where composites could be economically used in a variety of commercial industries. Today, airframe manufactures utilize composite materials in certain external areas such as wing flaps, elevators, rudders, spoilers, and landing gear doors [1].

As fabrication methods become even more economical, composites will be used more extensively as aircraft surface panel materials. With this increased use of composite materials on the exterior of aircraft, it is imperative that designer understand how these materials behave under all loading conditions. One of these loading conditions that exterior components will encounter throughout their service lives is impact loading due to foreign object impact. Because composites have poor resistance to damage due to out-of-plane impact, loading could preclude their use in some structures [2].

Hand lay-up is the most common and least expensive open-molding method because it requires the least amount of equipment. Fiber reinforcements are placed by hand in a mold and resin is applied with a brush or roller. Hand layup is an open molding method suitable for making a wide variety of composites products from very small to very large. Production volume per mold is low; however, it is feasible to produce substantial production quantities using multiple molds. Design changes are readily made. There is a minimum investment in equipment. With skilled operators, good production rates and consistent quality are obtainable [3].

Recently, there has been considerable interest in mechanical tests of fiber reinforced composites. BelingardiveVadori conducted a study on glass fiber epoxy resin composites low energy impact resistance and investigated energy absorbing ability at different impact velocities and deduced force-displacement graphs [4]. Different kinds of strikers affecting on the impact resistance of carbon epoxy composite laminates have recently been proposed in the literature by Mitrevski and colleagues; as a result, they have concluded that the samples exposed to impact by conic edge are the most energy absorbed sample [5]. Dimensional and striker effects to the low energy impact of composites have been investigated by Aslan and colleagues [6]. Milli and colleagues investigated the behaviors of epoxy glass composites at low velocity impact by using theoretical hertz impact law and obtained consistent results with the tests [7]. Karim and colleagues studied the impact behavior and performance of epoxy composites produced by under single and repeated low-velocity impact loading and showed that performance of epoxies decreases at low temperatures [8]. Kara investigated the dynamic behavior of epoxy glass composites under low velocity impact behavior and damage analysis

according to the different plate dimensions and obtained similar results as Karim and colleagues obtained [9]. Cho K. and friends studied the effect of heat fluctuations (low and high temperature) of impact damage on carbon fibers (CFRP) and obtained that heat fluctuations decreases impact resistance [10]. Ibekwe and colleagues have studied the damage effect of compression test on glass fiber reinforced composites at low temperature degrees [11]. T. Gomez and his colleagues examined the low impact damage behavior of CFRPs at different temperatures and concluded that the influence of temperature and ply reinforcement architecture of stacking sequence effect the mechanical behavior of the CFRP laminates subjected to low velocity impulsive loads [12]. Lal studied on the 8 layered isotropic graphite/epoxy composites low impact behavior [13]. Whittingham and colleagues investigated the low impact behavior of carbon fiber / epoxy laminates under prestress and depicted that penetration depth, impact load and absorbed energy are independent from prestress value upto 6J, but dependant at greater energy levels [14]. Husseinzadeh analyzed the high impact behavior of CFRPs numerically with ANSYS Ls-Dyna V6.1 software and obtained consistent results with experiments [15].

Also there has been studies and investigations on the impact behavior of composites at different temperature degrees; some of these studies are as follows:

Amin Salehi-Khojin and his colleagues investigated the role of temperature on impact properties of Kevlar/fiberglass composite laminates and showed that as the temperature decreases, strength decreases [16]. Jeremy Gustin and his colleagues studied on low velocity impact of combination kevlar/carbon fiber sandwich composites [17].

The originality of our study is based on the hand layup preparation and low velocity impact response analyze at low temperatures of CFRPs together. One group of samples for each array at 22,5°C have been subjected to test with strain-gauge. Also; strain analyze is conducted for this group.

## 2. MATERIAL AND METHOD

Carbon fiber and epoxy resin are used for preparation of plates (Table 1) by hand layup process at 23,7°C, % 28 humidity and under 650 mm Hg. pressure, approximately for 30 minutes. The plates have been vacuumed, after that they have been cured at 55°C for 16 hours [3].

The stacking sequence and numbers are depicted below:

Composite type: Carbon (CFU 10T), epoxy (CR 80) and CH 80-6 hardener (Fig. 1).

(%70 fiber-carbon-% 30 matrix-epoxy resin)

Dimension of samples : 100 x 100 mm.

Each layer thickness : 0,25 mm.

Plate thickness : 2 mm.



**Figure 1.** Composite plates after vacuum and curing process

**Table 1.** Properties of the constituents of plates [18, 19]

Properties	CFU 10T Carbon (fiber)	CR 80 Resin (epoxy)
Tensile strength (MPa)	1180	69
Tensile modulus (GPa)	190	3,2
Density (g/cm <sup>3</sup> )	1,8	1,17

**Table 2a.** Stacking sequence of samples

Sample Codes	Array
1N1(22,5°C strain gage), 1N2 (22,5°C), 1N3 (-30°C), 1N4 (-60°C), 1N5 (0°C),	[0/+45/+45/90] <sub>s</sub>
2N1(22,5°C strain gage), 2N2 (22,5°C), 2N3 (-30°C), 2N4 (-60°C), 2N5 (0°C),	[90/+45/0/-45] <sub>s</sub>
3N1(22,5°C strain gage), 3N2 (22,5°C), 3N3 (-30°C), 3N4 (-60°C), 3N5 (0°C),	[+45/0/-45/90] <sub>s</sub>

**Table 2b.** Stacking sequence of samples

Sample Codes	Array
4N1 (22,5°C strain gage), 4N2 (22,5°C), 4N3 (-30°C), 4N4 (-60°C), 4N5 (0°C),	[0/+45/90/-45] <sub>s</sub>
5N1 (22,5°C strain gage), 5N2 (22,5°C), 5N3 (-30°C), 5N4 (-60°C), 5N5 (0°C),	[0/-45/90/+45] <sub>s</sub>
6N1 (22,5°C strain gage), 6N2 (22,5°C), 6N3 (-30°C), 6N4 (-60°C), 6N5 (0°C),	[+45/0/90/-45] <sub>s</sub>

Samples (Table 1 and 2) have been prepared and tests have been carried out according to ASTM D7136 "Standard Test Method for Measuring the Damage Resistance of a Fiber-Reinforced Polymer Matrix Composite to a Drop-Weight Impact Event" [20].

A weight drop impactor test setup was used for impact tests (Fig. 2(a) and (b)). The device has been designed so as to make damage on the materials by a substance dropped from a definite height with low velocity and mass. For this study, all samples were impacted with a 9 kg. drop weight. Since, the drop weight was not changed, the different impact energies were achieved by adjusting the drop height. A pneumatic clamping fixture, with a 76.2 mm. (3in.) diameter opening, secured each sample during impact. The samples were impacted with a 12.7 mm. (0.5in.) diameter striker with a hemispherical tip, constructed by a high strength steel. Impulse software was used to display and store the impact data.

**Figure 2.** (a) Weight Drop Test Setup and Settlement of Sample to the Fixture

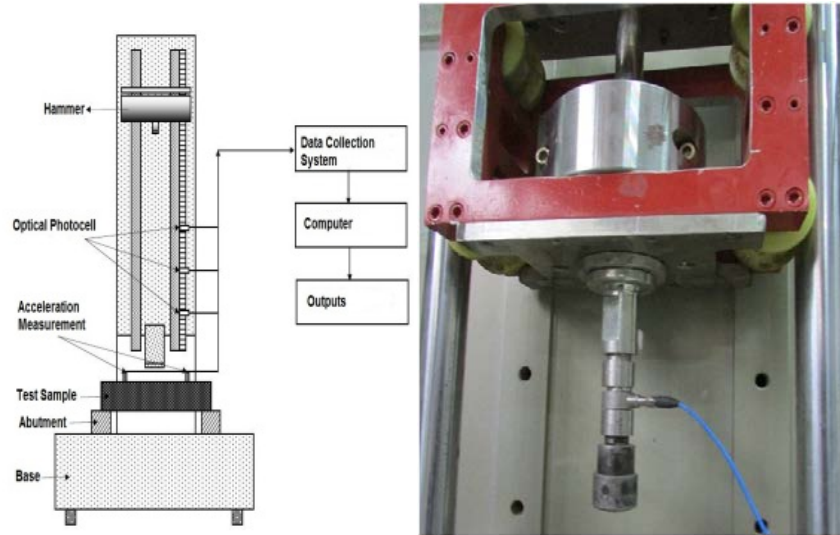


**Figure 2. (b)** Weight Drop Test Setup and Settlement of Sample to the Fixture

The force sensor 201B03 model (Table 3) ICP manufactured by PCB Group Company is used in tests (Fig. 3.)



**Figure 3.** The Force Sensor

**Table 3.** Technical Specification of Force Sensor

Specification	Value
Sensitivity	(±15%) 2248 mV/kN
Measuring Range (Pressure Force)	2,224 kN
Maximum Statical Force (Pressure Force)	13,34 kN
Broadband Resolution (1-10 000 Hz)	0,04448 N-rms
Low Frequency Response (-5%)	0,0003 Hz
Highest Frequency Limit	90 kHz

The data collector is the application that collects and delivers the metadata that is analyzed and presented in the GUI (Graphical user Interface) in computer (Table 4). The NI 9233-USB-9162 model data collector is used in tests (Fig. 4.)



**Figure 4.** NI 9233-USB-9162 Model Data Collector and Mounting

**Table 4.** Technical Specification of Data Collector

Specification	Value
Channel Number	4
Resolution	24-bite
Dynamic Interval	102 dB
Minimum Data Rate	2 kS/s
Maximum Data Rate	50 kS/s
Frequency	12,8 MHz
Sensitivity	$\pm 100$ ppm max.

Optical photocells are used in tests in order to measure the strain rate (Fig. 5.)

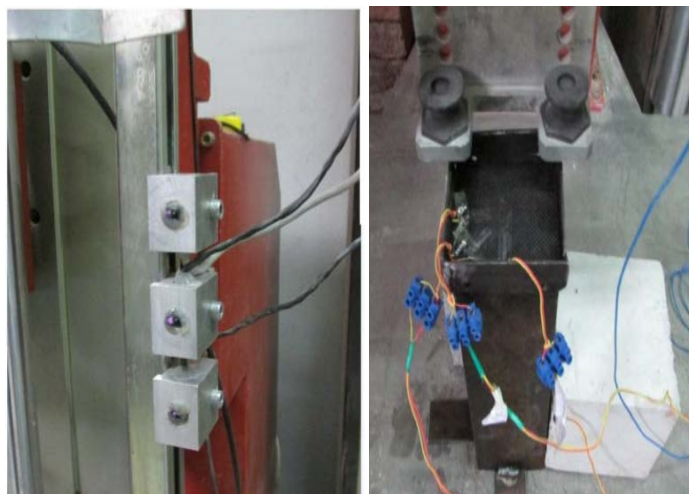


**Figure 5.** Optical photocells and sample with strain-gauges

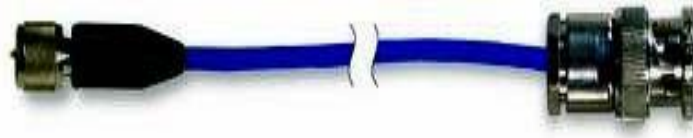


**Figure 6.** 003A20 Model LowNoise Coaxial Cable

Collected data from impact tests to the data collector was transmitted by coaxial cable without losing data (Fig. 6.).

Plates have been subjected to cooling operation by nitrogen gas and when desired temperature degree (0°C, -30°C and -60°C) is obtained, low velocity impact tests have been conducted immediately. The temperature degrees have been kept stable till the experiments were conducted (Fig.7).



**Figure 7.** Nitrogen Gas Tank

### 3. THE RESEARCH FINDINGS

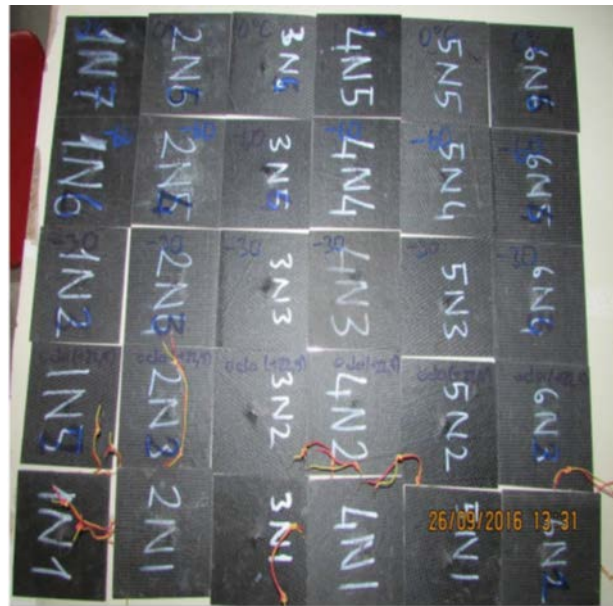


**Figure 8.** Samples subjected to low velocity impact test at +22,5 °C (strain gage), +22,5 °C, -30 °C, -60 °C and 0 °C respectively





**Figure 9.** *Samples with strain gage*

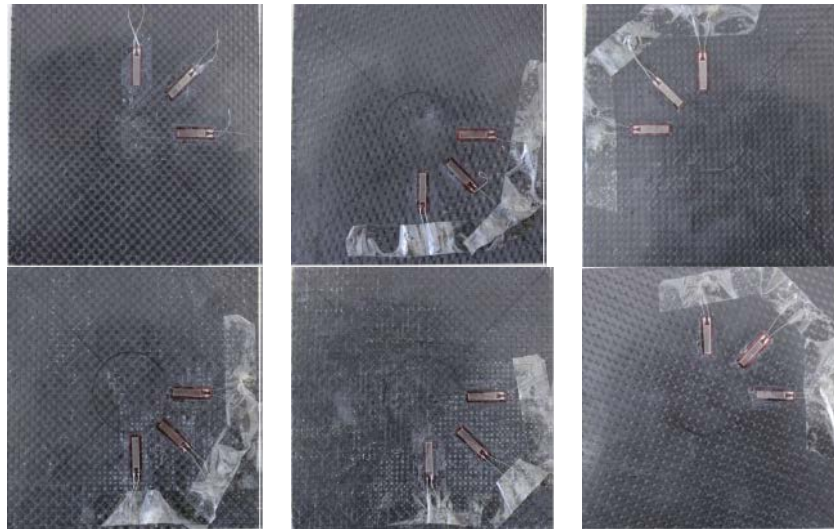


**Figure 10.** *Samples subjected to low velocity impact test at +22,5 °C (strain gage), +22,5 °C, -30 °C, -60 °C and 0 °C respectively*

A Strain gage (sometimes referred to as a Strain Gauge) is a sensor whose resistance varies with applied force; it converts force, pressure, tension, weight, etc., into a change in electrical resistance which can then be measured. When external forces are applied to a stationary object, stress and strain are the result. Stress is defined as the object's internal resisting forces, and strain is defined as the

displacement and deformation that occur. Strain gauges (120 ( $\Omega$ ) and % 3 strain limit) are used to measure the strain for the samples that have been subjected to impact at +22,5°C (fig.9 ve 10). [21].

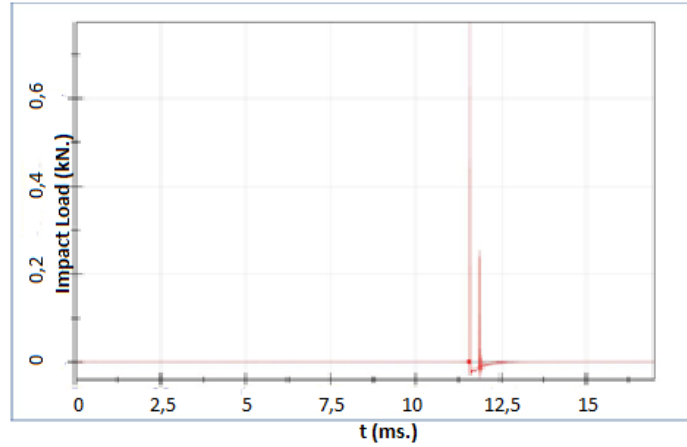


**Figure 11.** Signals taken by samples subjected to repeated forces

Until striking edge hits the sample, force is zero. Just at the hitting time, the force increases to a very high level and then again after second hit a small force magnitude has been obtained compared to the first hit as seen in Fig. 11. This means a second impact force has been applied. And as seen in Fig. 12., after second impact force a less contact force has been observed. Until the striking end stops, the impact forces continues. For force is the initiating force that makes a permanent damage.

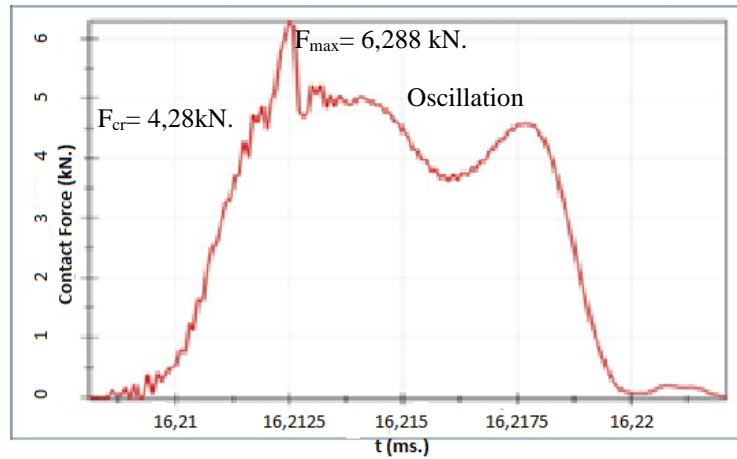


**Figure 12.** Force-time graph of [0/+45/-45/90] oriented sample subjected to low velocity impact test (strain-gauge mounted)

**Table 5.** Impact Parameters

Impactor (Striker) Diameter(mm.)	76,2 mm.
Impact Velocity (m/s.) (upon impact)	2,44 m/s.
Mass of Impactor (kg.)	9 kg.
Impact Energy (J.)	26,5 J
Impactor Height to Sample (mm.)	300 mm.

**Table 6.** The results obtained from  $[0/+45/+45/90]$  oriented sample subjected to low velocity impact test (strain-gauge mounted)

$F_{max}$ (kN)	$F_{cr}$ (kN)	$t_{Fmax}$ (ms.)	$t_{total}$ (ms.)
6,288	4.28	0.0019	0.014

$F_{max}$  : Maximum force obtained

$F_{cr}$  : Critical force initiating damages at the samples.

$t_{Fmax}$  : time for  $F_{max}$

$t_{total}$  : total impact time

Impact parameters are depicted at Table 5.

The first damage starts to occur in the sample at  $F_{cr}$ , (fig.10). This is called as  $F_{cr}$  (critical force starting to cause damages at the samples). Then the force reach to a maximum, after that an oscillation is observed until a second  $F_{max2}$ . Contact force decreases sharply to 0 (zero) as observed in  $[0/+45/+45/90]$  oriented sample subjected to low velocity impact test (strain-gauge mounted) (Table 6 and Fig.12). For a non-reversible and visible damage,  $F_{cr}$  must be exceeded. If not, invisible damages could be observed.

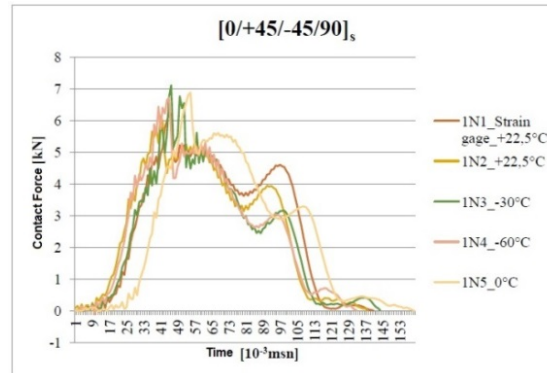


**Figure 13.** Contact force -time graph of  $[0/+45/+45/90]_s$  (Sample code 1N) oriented samples subjected to low velocity impact test at different temperatures

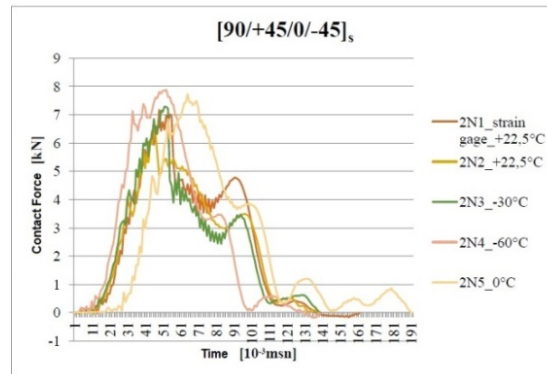


**Figure 14.** Contact force -time graph of  $[90/+45/0/-45]_s$  (Sample code 2N) oriented samples subjected to low velocity impact test at different temperatures.

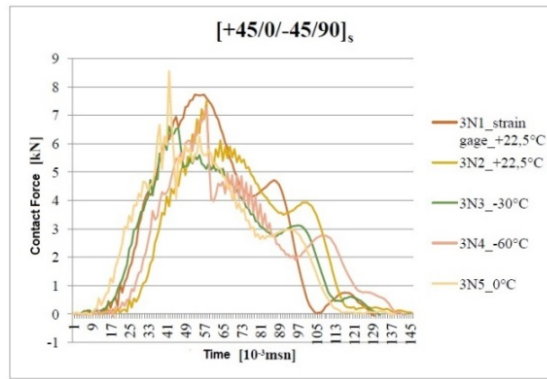


**Figure 15.** Contact force -time graph of [+45/0/-45/90]<sub>s</sub> (Sample code 3N) oriented samples subjected to low velocity impact test at different temperatures

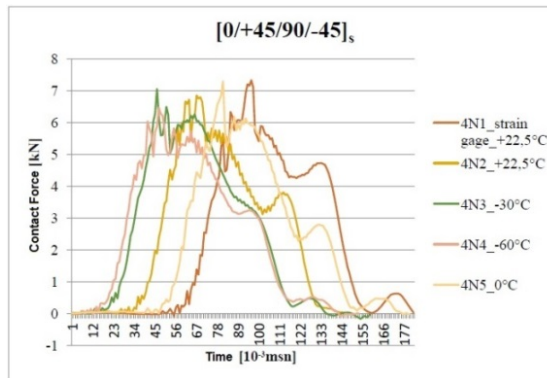


**Figure 16.** Contact force -time graph of [0/+45/90/-45]<sub>s</sub> (Sample code 4N) oriented samples subjected to low velocity impact test at different temperatures

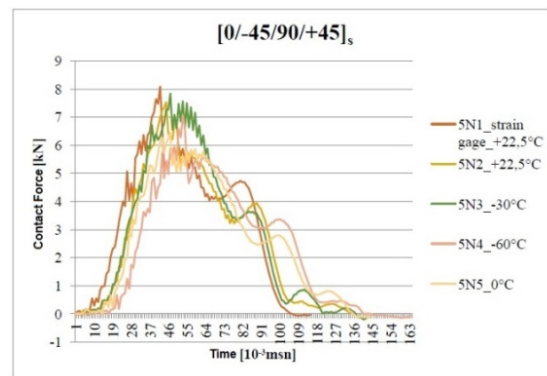


**Figure 17.** Contact force-time graph of [0/-45/90/+45]<sub>s</sub> (Sample code 5N) oriented samples subjected to low velocity impact test at different temperatures

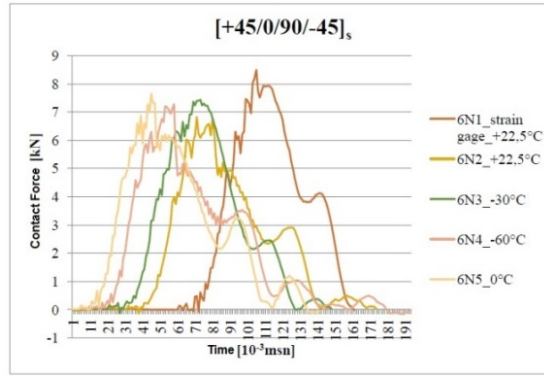


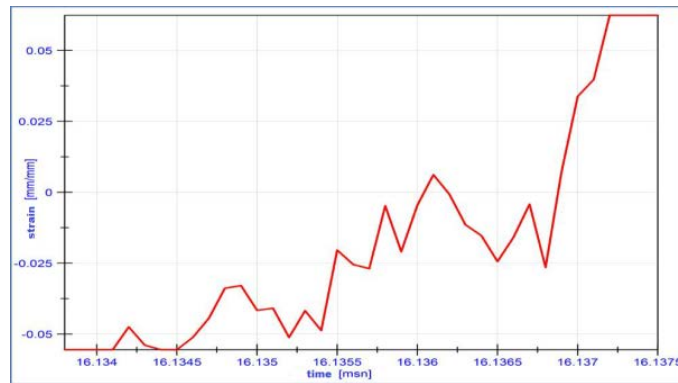
**Figure 18.** Contact force -time graph of [+45/0/90/-45]<sub>s</sub> (Sample code 6N) oriented samples subjected to low velocity impact test at different temperatures

**Table 7.** Contact Force-Time Values According to Fig.11-16 ( $t_{start}$  is 0 (second) for all samples)

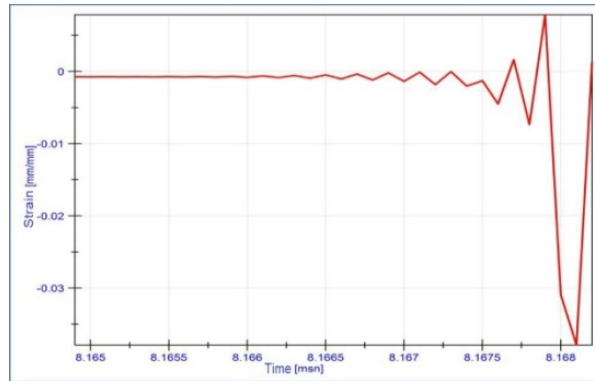
Sample Number	$t_{Fmax}$ (ms.)	$t_{total}$ (ms.)
1N1	4,4	14
1N2	4	13,7
1N3	4,5	14,3
1N4	4,4	13,2
1N5	5,4	15,9
2N1	5,4	16,1
2N2	4,5	13,8
2N3	4,5	13,9
2N4	5,2	13,9
2N5	6,9	19,1
3N1	5,6	12,9
3N2	5,7	14,5
3N3	4,1	13,1
3N4	5,7	14,2
3N5	4,1	13,8
4N1	9,5	18,1
4N2	6,6	14,5
4N3	4,5	15,8
4N4	4,6	15,2
4N5	8	17,9
5N1	4,1	11,4
5N2	4,4	13,4
5N3	4,6	14,2
5N4	5,2	16,3
5N5	4,6	14,3
6N1	10,5	16,1
6N2	7,1	17,4
6N3	7,3	14,8
6N4	5,8	19,3
6N5	4,5	14,1

$F_{\text{contact}}$  is the reaction force to the impact force,  $F_{\text{cr}}$  force is the initiating force that makes a permanent damage and  $F_{\text{max}}$  is the ultimate force that sample reacts to the impact force as seen in fig.13 through fig.18.

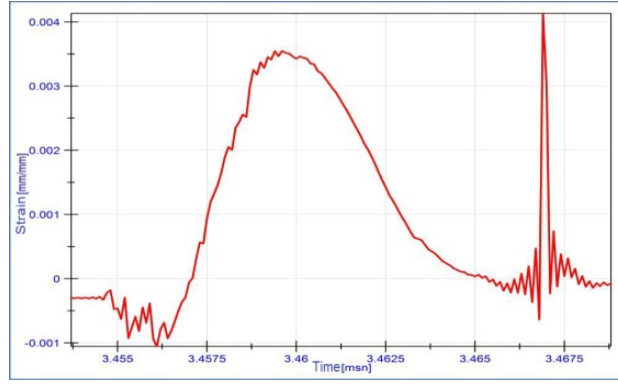
As temperature increases, delamination occurs at all layers. This result indicates the decreasing of stiffness. In other words impact strength decreases, as temperature decreases. In 1,2,4 and 5 numbered samples that starting in with  $0^\circ$  and  $90^\circ$  oriented angles, delamination occurs almost at all layers. In 3 and 6 numbered samples that starting in with  $+45^\circ$  oriented angles, delamination mostly occurs at substrates, as a result it can be deduced that samples starting in with  $+45^\circ$  oriented angles have more strength than the other ones. Reset time is utmost at 6N4 number sample ( $-60^\circ\text{C}$ ), it means the most resilient one is this sample among the other ones. As the temperature decreases, damage area increase. Low temperature significantly effects the damage areas (Table 7).



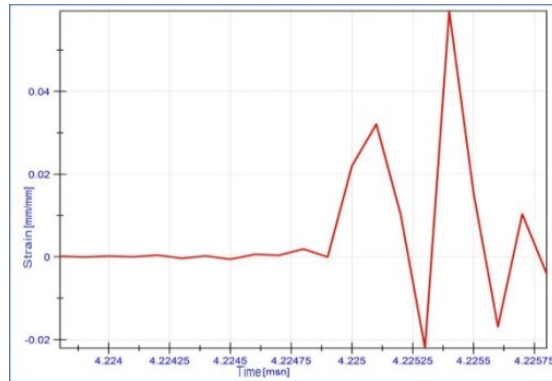
(a)  $[0/+45/+45/90]_s$



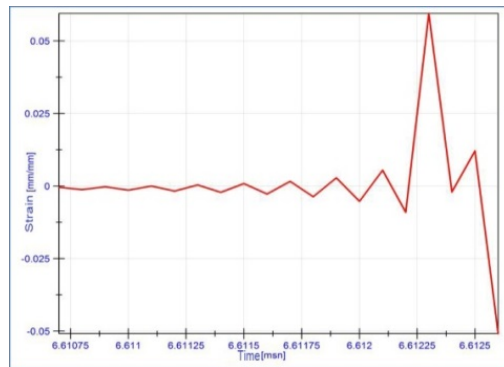
(b)  $[90/+45/0/-45]_s$



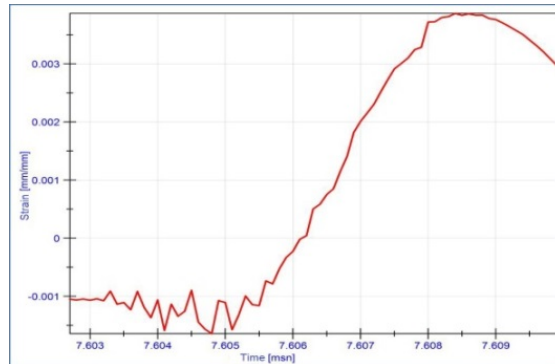
(c) [+45/0/-45/90]s



(d) [0/+45/90/-45]s



(e) [0/-45/90/+45]s



(f) [+45/0/90/-45]s

**Figure 19.** Strain-time graphs of samples subjected to low velocity impact test at different temperatures a) 1N1, b) 2N1, c) 3N1, d) 4N1, e) 5N1, f) 6N1 (strain gauge mounted samples at 22,5°C)

Strain amount is high at the  $[0/+45/-45/90]_s$  oriented sample and damage area less. Strain amount is low at the  $[+45/0/90/-45]_s$  oriented sample and damage area is more.  $[0/+45/90/-45]_s$  and  $[0/-45/90/+45]_s$  oriented samples area identical to each other so strain values is almost same (Fig. 17). It is observed that if the damage occurs earlier, material has lower toughness and more brittle; and vice versa. The reason why the strain values begin under zero is the compression force observed during impact force applied to the samples.

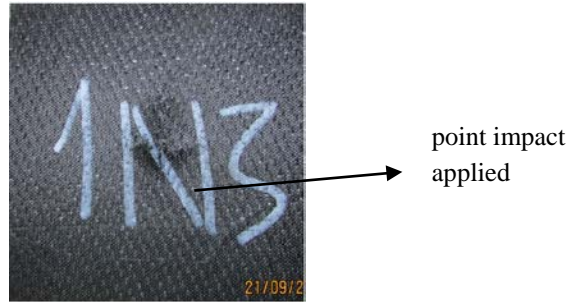


**Figure 20.** *Impact Applied Point*

Impact force is applied directly to the center of samples (fig.20).

Damage photos (fig. 21 through fig 26. for 1N1, 2N1, 3N1, 4N1, 5N1 and 6N1) observed under microscopy could be seen for all samples from Fig. 27 to Fig. 32.

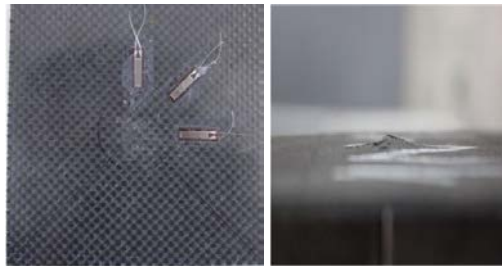


**Figure 21.** *Impact Applied Point (1N1 Sample)*



**Figure 22.** *Impact Applied Point (2N1 Sample)*



**Figure 23.** *Impact Applied Point (3N1 Sample)*



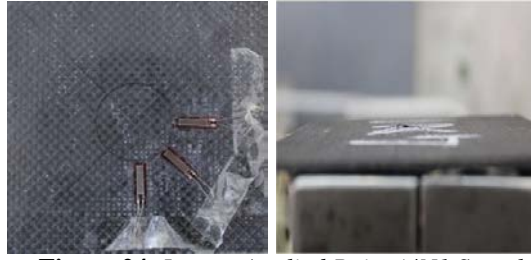


**Figure 24.** *Impact Applied Point (4N1 Sample)*

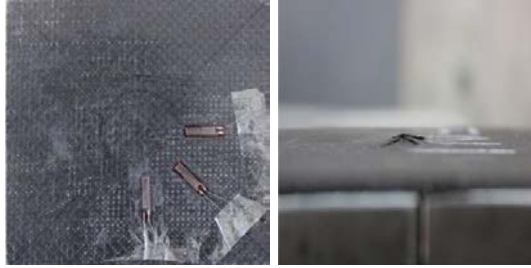


**Figure 25.** *Impact Applied Point (5N1 Sample)*



**Figure 26.** *Impact Applied Point (6N1 Sample)*

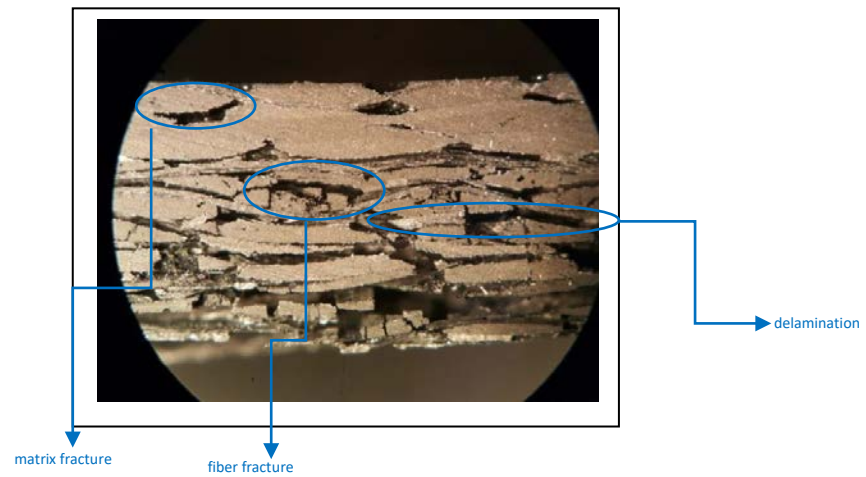


**Figure 27.** *Cross section view of 1N1 sample under microscopy (1N2, 1N3, 1N4 and 1N5 samples damages are same as 1N1 with very little differences, so they are not depicted in here.)*

As it is observed at the [0/+45/-45/90]s array;

(1N1); delamination is more at substrates, matrix fractures are more at top 3 layers. Fiber fracture is mostly observed at bottom 2 layers.

(1N2); matrix fractures and delamination are observed almost at all layers, fiber fracture is mostly observed at bottom 2 layers.

(1N3); delamination is observed at bottom 4 layers, fiber fractures are more at bottom 2 layers. Matrix fractures are mostly observed at interstages intensely.

(1N4); delamination is observed at bottom 4 layers, matrix fractures are observed after 2nd layer. Fiber fractures are mostly observed at bottom 2 layers.

(1N5); matrix fractures are observed at top 3 layers intensely, fiber fractures are observed at bottom 2 layers. Delamination occurs after 2nd layer.

Generally; fiber fractures are observed at -45° and 90° angle layers, matrix fractures and delaminations occur at 0° and 45° angle layers. Most delamination is observed at 1N4 sample (-60 °C), the least at 1N3 sample (-30 °C).

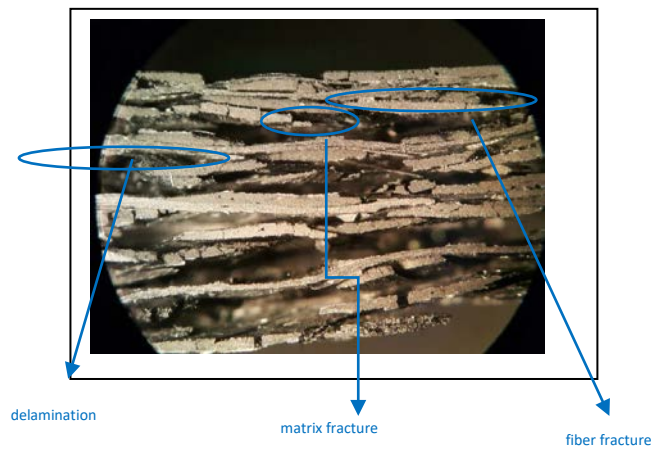


**Figure 28.** Cross section view of 2N1 sample under microscopy (2N2, 2N3, 2N4 and 2N5 samples damages are same as 2N1 with very little differences, so they are not depicted in here.)

As it is observed at the [90/+45/0/-45]s array;

(2N1); matrix fractures are observed almost at all layers with delamination, fiber fracture is mostly observed at bottom layers.

(2N2); matrix fractures and delamination are observed, fiber fracture is mostly observed at bottom layers.

(2N3); delamination and fiber fractures are mostly observed at bottom layers, matrix fractures at top layers and delamination are observed in patches at top layers.

(2N4); matrix fractures and delamination are observed at all layers, fiber fracture is observed at bottom layers.

(2N5); matrix fractures and delamination are observed, fiber fracture is observed at bottom 3 layers.

Generally; fiber fractures are observed at  $-45^\circ$  angle orientation layers, matrix fractures at  $90^\circ$  angle and delaminations occurs at  $0^\circ$  and  $45^\circ$  angle orientation layers. Most delamination is observed at 2N4 sample ( $-60^\circ\text{C}$ ), the least at 2N1 sample ( $22,5^\circ\text{C}$ ).

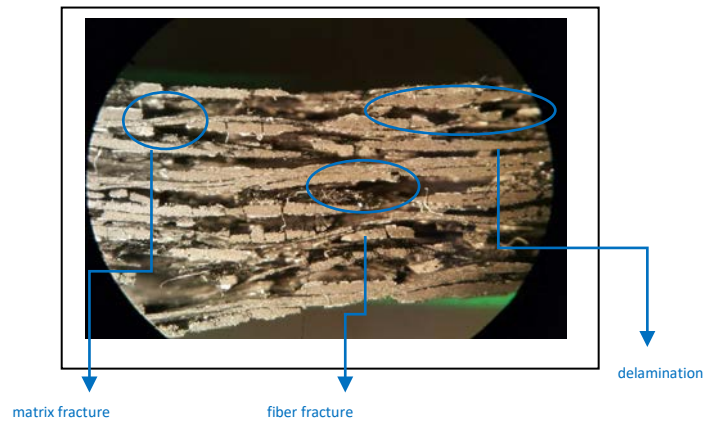


**Figure 29.** Cross section view of 3N1 sample under microscopy (3N2, 3N3, 3N4 and 3N5 samples damages are same as 3N1 with very little differences, so they are not depicted in here.)

As it is observed at the [+45/0/-45/90]s array; (3N1); matrix fractures are observed almost at all layers with delamination, fiber fracture is mostly observed at bottom 2 layers.

(3N2); matrix fractures and delamination are observed after 2<sup>nd</sup> layer, fiber fracture is mostly observed at 2 bottom layers.

(3N3); matrix fractures and delamination are observed after 3<sup>rd</sup> layer, fiber fracture is mostly observed at 2 bottom layers.

(3N4); matrix fractures are observed almost at all layers with delamination, fiber fracture is mostly observed at first layer and bottom 2 layers.

(3N5); matrix fractures and delaminations are observed, fiber fracture is mostly observed at bottom 2 layers.

Generally; fiber fractures are observed at  $-45^\circ$  and  $90^\circ$  angle orientation layers, matrix fractures and delaminations occur at  $0^\circ$  and  $-45^\circ$  angle orientation layers. Fiber fracture at the first layer of samples is only observed at 3N4 ( $-60^\circ\text{C}$ ), number sample. Most delamination is observed at 3N4 sample ( $-60^\circ\text{C}$ ), the least at 3N3 sample ( $-30^\circ\text{C}$ ).

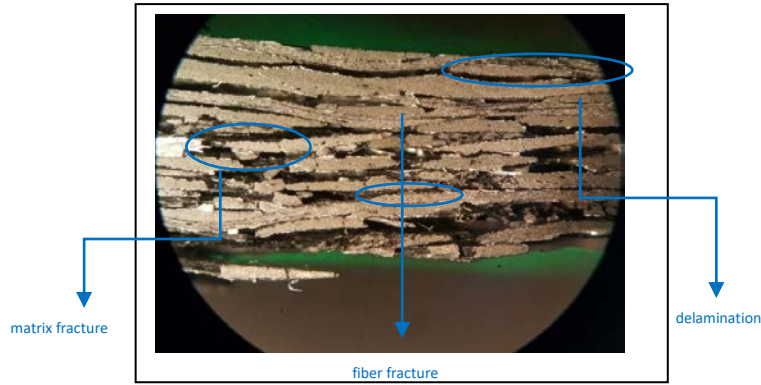


**Figure 30.** Cross section view of 4N1 sample under microscopy (4N2, 4N3, 4N4 and 4N5 samples damages are same as 4N1 with very little differences, so they are not depicted in here.)

As it is observed at the  $[0/+45/90/-45]_s$  array;

(4N1); matrix fractures are observed almost at all layers with delamination, fiber fracture is mostly observed at bottom 2 layers.

(4N2); matrix fractures are observed heavily at all layers with delamination, fiber fracture is mostly observed at bottom 2 layers.

(4N3); matrix fractures are observed after 2<sup>nd</sup> layer with delamination, fiber fracture is mostly observed at bottom 2 layers.

(4N4); matrix fractures are observed almost at all layers with delamination, fiber fracture is mostly observed at bottom 2 layers.

(4N5); matrix fractures are observed heavily at all layers with delamination, fiber fracture is mostly observed at top 2 and bottom 4 layers.

Generally; fiber fractures are observed at  $0^\circ$ ,  $-45^\circ$  and  $90^\circ$  angle orientation layers, Matrix fractures and delaminations occur at  $0^\circ$ ,  $+45^\circ$  and  $90^\circ$  angle orientation layers. Most delamination is observed at 4N3 sample ( $-30^\circ\text{C}$ ), the least at 4N2 sample ( $22,5^\circ\text{C}$ ).

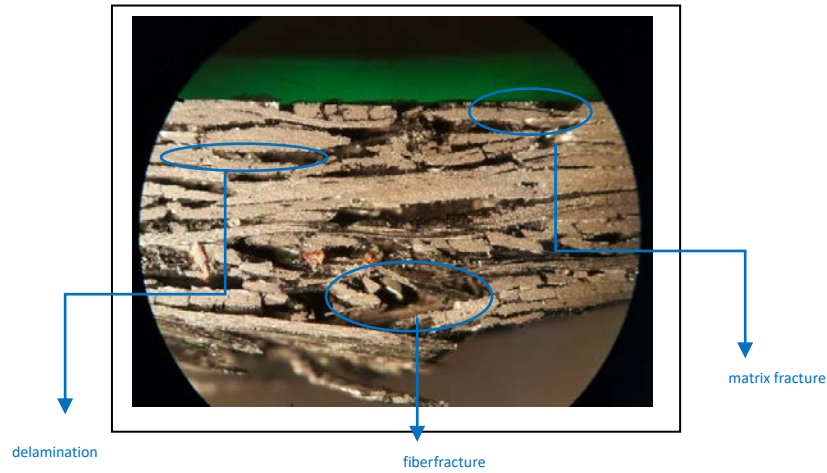


**Figure 31.** Cross section view of 5N1 sample under microscopy (5N2, 5N3, 5N4 and 5N5 samples damages are same as 5N1 with very little differences, so they are not depicted in here.)

As it is observed at the [0/-45/90/+45]s array;

(5N1); matrix fractures are observed heavily almost at all layers with delamination, fiber fracture is mostly observed at bottom 3 layers.

(5N2); matrix fractures are observed at all layers with delamination, fiber fracture is mostly observed at bottom 3 layers.

(5N3); matrix fractures are observed heavily almost at all layers with delamination, fiber fracture is mostly observed at bottom 3 layers.

(5N4); matrix fractures are observed after 2<sup>nd</sup> layer with delamination, fiber fracture is mostly observed at bottom 3 layers.

(5N5); matrix fractures are observed heavily almost at all layers with delamination, fiber fracture is mostly observed at bottom 3 layers.

Generally; fiber fractures are observed at  $\pm 45^\circ$  and  $90^\circ$  angle orientation layers, matrix fractures and delaminations occurs at  $0^\circ$ ,  $\pm 45^\circ$  and  $90^\circ$  angle orientation layers. Most delamination is observed at 5N5 sample ( $0^\circ\text{C}$ ), the least at 5N2 sample ( $22,5^\circ\text{C}$ ).

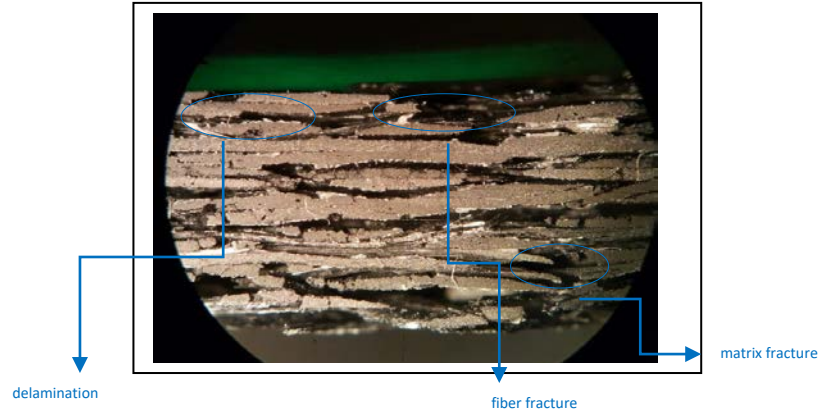


**Figure 32.** Cross section view of 6N1 sample under microscopy (6N2, 6N3, 6N4 and 6N5 samples damages are same as 6N1 with very little differences, so they are not depicted in here.)

As it is observed at the [+45/0/90/-45]<sub>s</sub> array;

(6N1); matrix fractures are observed at all layers with delamination, fiber fracture is mostly observed at bottom 2 layers.

(6N2); matrix fractures are observed at all layers with delamination, fiber fracture is mostly observed at bottom 2 layers.

(6N3); matrix fractures are observed after 3<sup>rd</sup> layer with delamination, fiber fracture is mostly observed at bottom 2 layers.

(6N4); matrix fractures are observed at all layers with delamination, fiber fracture is mostly observed at bottom 2 layers.

(6N5); matrix fractures are observed at all layers with delamination, fiber fracture is mostly observed at bottom 2 layers.

Generally; fiber fractures are observed at -45 ° and 90° angle orientation layers, matrix fractures and delaminations occurs at 0 °, +45 ° and 90° angle orientation layers. Most delamination is observed at 6N3 sample (-30 °C), the least at 6N1 sample (22,5 °C).

**Table 8.**  $F_{contact}$  - Strain and Deflection Amount in All Samples

Sample Code	Temperature (°C)	F (kN)	Strain (mm./ mm)	Deflection (mm.)
1N1 (Strain gage)	+22,5°C	6,288	0,0624	2,35
1N2	+22,5°C	6,1531		2,425
1N3	-30°C	7,117		2,29
1N4	-60°C	6,729		3,615
1N5	0°C	6,8878		3,53
2N1 (Strain gage)	+22,5°C	7,171	0,00784	2,23
2N2	+22,5°C	6,446		3,49
2N3	-30°C	7,2874		3,55
2N4	-60°C	7,885		4,925
2N5	0°C	7,732		3,525
3N1 (Strain gage)	+22,5°C	7,732	0,00413	3,50
3N2	+22,5°C	7,499		2,15
3N3	-30°C	6,6133		2,255
3N4	-60°C	7,289		3,95
3N5	0°C	8,563		3,485
4N1 (Strain gage)	+22,5°C	7,33116	0,0594	3,385
4N2	+22,5°C	6,853		2,15
4N3	-30°C	7,056		3,765
4N4	-60°C	6,467		3,70
4N5	0°C	7,293		3,73
5N1 (Strain gage)	+22,5°C	8,091	0,0594	3,79
5N2	+22,5°C	7,533		2,39
5N3	-30°C	7,845		3,50
5N4	-60°C	7,070		3,80
5N5	0°C	6,452		3,855
6N1 (Strain gage)	+22,5°C	8,4945	0,00386	2,025
6N2	+22,5°C	6,826		2,89
6N3	-30°C	7,4358		3,93
6N4	-60°C	7,281		3,91
6N5	0°C	7,652		3,58

As seen in table 8; the sequence stack and temperature degress has no certain effect on the impact performance of samples; but we can generally say that deflection at low temperatures is more. This is also a significant outcome of the study according to the test results.

#### 4. DISCUSSION

As the temperature decreases, it could be obviously seen all kinds of damage failures (fiber-matrix fracture and delamination) from Fig. 18 through 23. Delamination is observed in all layers, as strength decreases. As the temperature decreases, impact resistance decreases, and damage quantity increases.

1,2,4 and 5 numbered samples beginning with 0 ° and 90 ° angles have delamination after impact almost at all layers. Samples beginning with +45° orientation angles (number 3 and 6 samples) ,delamination has been observed mostly at lower layers. Samples beginning with +45° angles have

better impact resistance than the other samples. This is an important result that can be obtained from our study.

As the temperature decreases, the strength of matrix (epoxy) also decreases. So matrix fracture could be observed. As matrix fracture occurs, fiber cleavages fractures and delaminations have been triggered (Fig. 18-23). And also fiber fractures triggers matrix fractures. This is the second important result observed; so the failure in the samples should be considered as a whole; this phenomenon is free from temperature or array of samples. This is the third important result that is concluded from the study.

The force-time graphs for all samples could be seen Fig. 11 through Fig. 16. First of all there is an abrupt increase in force versus time, then a small oscillation and then slowly decrease. As oscillation increases, damage decreases. Also as temperature increases, oscillation increases. This lead us to a conclusion that free from fiber and matrix array; as temperature decreases, damage quantity increases and as temperature increases, tougher structure could be observed. This means less damage area. Damage area has been observed through the microscope (optic microscope) in all the samples and evaluated as fiber, amtrix fracture or delamination [2].

This result also could be seen in strain-time graphs (fig.17). As temperature decreases, strain decreases and more damage area could be observed. More delamination, matrix and fiber fracture areas can be as temperature decreases. This is the most important observed and experimental result of this project; in other words as strain increases, damage amount decreases.

Fiber and layer orientation is an important factor at CFRP damage behaviors in temperature and force applied. At lower temperatures interlaminar residual stress affects matrix fracture as well as delamination.

As strain increases, damage quantity decreases. Strain amount has a retarding effect on matrix and fiber fracture. It is observed and experimentally seen that the strain is inversely proportional to damage quantity.

## 5. CONCLUSION

Low impact response at low temperatures of CFRP platesfabricated by hand layup method have been investigated. As well as temperature; failure behaviors of different arrayed plates and strain behavior at 22,5°C have been observed. Preparation of samples, implementation of test setup and connection of strain-gauges have been done. Following results can be concluded;

1. It has been observed experimentally that +45° and -45° arrays ( 3N and 6N) have better strength values than +90° and -90° arrays (1N,2N,4N and 5N).



2. As the temperature decreases, the strength decreases.
3. In all damaged CFRPs samples; delamination, fiber and matrix fracture have been observed.
4. Damages affected by compression forces are less than tensile forces.
5. Damages at rear side of samples are much more than the front side because of the tensile forces.
6. 1,2,4 and 5 numbered samples beginning with 0 ° and 90 ° angles have more strain values than 3 and 6 numbered samples beginning with +45 ° orientation angles, this means samples beginning with +45° angles have better impact resistance than the other samples (number 1,2,4 and 5 samples), because  $F_{cr}$  is higher as proved experimentally (fig.13-18).

### CONFLICTS OF INTEREST

No conflict of interest was declared by the authors.

### REFERENCES

- [1] T.J. Reinhart, L.L. Clements, Introduction to Composites, Engineered Materials Handbook Volume 1, ASM International, Ohio, 1987
- [2] B.D Agarwall, L. J. Broutman, Analysis and Performance of Fiber Composites, Wiley-Interscience, New York,1980.
- [3] W.J. Stuart, Composite Materials Lay Up Lab Lecture Notes, Edmonds Community College, Washington, 2010.
- [4] G. Belingardi, R. Vadori, Low velocity impact tests of laminate glass-fiber-epoxy matrix composite material plates, Internal Journal of Impact Engineering 27 (2002) 213-229.
- [5] T.Mirevski, I.H. Marshall, R. Thomson, The influence of impactor shape on the damage to composite laminates, Journal of Composite Structures 76 (2006) 116-122.
- [6] Z. Aslan, R. Karakuzu, B. Okutan, The response of laminated composite plates under low-velocity impact loading, Journal of Composite Structures 59 (2003) 119-127
- [7] F. Milli, B. Necib, Impact behavior of cross-ply laminated composite plates under low velocities, Journal of Composite Structures 51 (2001) 237-244.
- [8] M.V. Hoşur, M.R. Karim, S. Jeelani, Experimental investigations on the response of stitched/unstitched woven S2-glass/SC15 epoxy composites under single and repeated low-velocity impact loading, Journal of Composite Structures 61 (2003) 89-102.
- [9] M. Kara, Dynamic Response Of Low Velocity Impact Composite, Selçuk University, Institute Of Science and Technology, Konya, 2006 Ms.S. Thesis.
- [10] K. Cha, O. Kim, S. Yang, Affects of temperature on impact damages in CFRP composite laminates, Journal of Composite Structures 32 (2001) 669-682.
- [11] S.J. Ibekwe, P. Mensah, S. Pang, M. Stubblefield, Impact and post impact response of laminated beams at low temperatures, Journal of Composite Structures 79 (2007) 12-17
- [12] T. Gomez del Rro, R. Zaera, E. Barbero, C. Navarro, Damage in CFRP due to low velocity impact at low temperature, Composite Engineering 36 (2005) 41-50.
- [13] K.M. Lal, Prediction of residual tensile strength of transversely impacted composite laminates, Structure Solid Mechanics NASA CP-2245 (1982) 97-111.

- [14] B. Whittingham, I.H. Marshall, T. Mitrevski, R. Jones, The response of composite structures with pre-stress subject to low velocity impact damage, *Composite Structures* 66 (2004) 685-698.
- [15] R. Husseinzadeh, M.M. Shokrieh, L. Lessard, Damage behaviour of fiber reinforced composite plates subjected to drop weight impact, *Composite Science and Technology* 66 (2006) 61-68.
- [16] S.K. Amin, B. Reza, M. Mohammad, N.J. Reza, The Role of Temperature on Impact Properties of Kevlar/fiberglass, *Composites Part B. Elsevier* 37 (2006) 593-602.
- [17] G. Jeremy, J. Aaran, M. Mohammod, S. James, Low Velocity Impact Combination Kevlar/Carbon Fiber Sandwich Composites, *Composite Structures. Elsevier Composites* 69 (2005) 396-406.
- [18] Product Technical Information, Dowaksa. 2019. (Date to Access: 01.09.2019) <http://www.dowaksa.com/wp-content/uploads/2016/08/TDS-CFU10T-Carbon-Fabric.pdf>
- [19] Product Technical Information, Compositeshop.de, 2019. (Date to Access: 01.09.2019) <https://www.compositeshop.de/xoshop/files/Biresin-CR80.pdf>
- [20] ASTM D7136, Standard Test Method for Measuring The Damage Resistance Of A Fiber-Reinforced Polymer Matrix Composite To A Drop Weight Impact Event, American Society For Testing and Materials, New York, 2005.
- [21] Technical Information, Omega Engineering-Czech, 2019, <https://www.omegaeng.cz/prodinfo/straingages.html> (Date to Access: 01.09.2019)